

EFFECT OF N-METHYL-D-ASPARTATE RECEPTOR BLOCKADE ON PLASTICITY OF FRONTAL CORTEX AFTER CHOLINERGIC DEAFFERENTATION IN RAT

J. E. GARRETT,^{a,b} I. KIM,^a R. E. WILSON^{a,b}
AND C. L. WELLMAN^{a,b*}

^aDepartment of Psychological and Brain Sciences, Indiana University, Bloomington, IN 47405, USA

^bProgram in Neuroscience, Indiana University, Bloomington, IN 47405, USA

Abstract—Cholinergic projections from the nucleus basalis play a critical role in cortical plasticity. For instance, cholinergic deafferentation increases dendritic spine density and expression of the GluR1 subunit of the α -amino-3-hydroxy-5-methylisoxazole-4-propionate receptor in frontal cortex. Acetylcholine modulates glutamatergic activity in cortex, and the *N*-methyl-D-aspartate subtype of glutamate receptor plays a role in many forms of synaptic plasticity. To assess whether *N*-methyl-D-aspartate receptors mediate the increase in GluR1 and spine density resulting from cholinergic deafferentation, we examined the effect of *N*-methyl-D-aspartate receptor blockade on nucleus basalis lesion-induced upregulation of GluR1 and dendritic spines. Rats received unilateral sham or 192 IgG saporin lesions of the nucleus basalis. Half of the rats in each group were treated with the *N*-methyl-D-aspartate antagonist MK-801 or phosphate-buffered saline. Two weeks later, brains were processed for either immunohistochemical staining of the GluR1 subunit or Golgi histology. In layer II–III of frontal cortex, neuronal GluR1 expression was assessed using an unbiased stereological technique, and spine density was assessed on basilar branches of pyramidal neurons. GluR1 expression was increased after nucleus basalis lesion, but this increase was prevented with MK-801. Similarly, nucleus basalis-lesioned animals had significantly higher spine densities, and this effect was also prevented by treatment with MK-801. Thus, *N*-methyl-D-aspartate receptor blockade prevented both GluR1 and spine density upregulation following cholinergic deafferentation, suggesting that these effects are *N*-methyl-D-aspartate receptor-mediated. © 2006 Published by Elsevier Ltd on behalf of IBRO.

Key words: acetylcholine, AMPA, basal forebrain, motor cortex, glutamate, dendritic spine.

The nucleus basalis magnocellularis (NBM) is a basal forebrain cholinergic nucleus with specific and direct projections to frontal cortex (Johnston et al., 1981; Bigl et al., 1982). Acetylcholine supplied by the NBM modulates neo-

cortical function (Rasmusson and Dykes, 1988; Kurosawa et al., 1989; Tremblay et al., 1990a,b; Webster et al., 1991) and cortical plasticity. For instance, lesions of the NBM postnatally disrupt cortical development (Hohmann et al., 1988; Ricceri et al., 2002), and in adulthood alter dendritic morphology in frontal cortex (Works et al., 2004) and prevent reorganization of somatosensory cortex following nerve transection (Juliano et al., 1991; Webster et al., 1991). Other evidence suggests a role for cholinergic projections to the neocortex in synaptic plasticity: blockade of cortical muscarinic receptors prevents LTP in layer II–III neurons in frontal cortex (Hess and Donoghue, 1999). Finally, cholinergic deafferentation increases spine density on basilar dendrites of layer II–III pyramidal neurons (Harmon and Wellman, 2003).

Acetylcholine supplied by the NBM acts as a neuro-modulator at glutamatergic synapses in the neocortex, increasing glutamate-evoked excitation when iontophoretically applied (e.g. Metherate et al., 1987; e.g. Tremblay et al., 1990a). Glutamate is the major excitatory neurotransmitter in neocortex (Puil and Benjamin, 1988), and has been implicated in the development and maintenance of dendritic morphology (Mattson et al., 1988; Wilson and Keith, 1998). Moreover, the α -amino-3-hydroxy-5-methylisoxazole-4-propionate (AMPA) subtype of glutamate receptor appears to mediate the effects of glutamate on dendritic morphology: blockade of AMPA/kainate receptors alters morphology of developing neurons (Metzger et al., 1998; Wong et al., 2000), and overexpression of the GluR1 subunit of the AMPA receptor alters dendritic morphology at maturity (Inglis et al., 2002). Furthermore, AMPA receptors are localized in the vast majority of dendritic spines (Kennedy, 2000). Thus, lesion-induced increases in spine density could reflect changes in AMPA receptor expression in frontal cortex. Indeed, NBM lesion-induced increases in AMPA receptor binding have been demonstrated using quantitative autoradiography (Roβner et al., 1995; Wellman and Pellemounter, 1999). Finally, cholinergic deafferentation increases the number of intensely GluR1-immunopositive neurons in layer II–III of frontal cortex of young adult rats (Kim et al., 2005). Thus, cholinergic deafferentation produces increases in both spine density and AMPA receptor protein in layer II–III neurons in frontal cortex.

The *N*-methyl-D-aspartate (NMDA) subtype of glutamate receptors also plays a role in synaptic plasticity. For example, cortical reorganization following nerve transection is dependent on NMDA receptors (Garraghty and Muja, 1996), and the upregulation of both AMPA receptors

*Correspondence to: C. L. Wellman, Department of Psychological and Brain Sciences, Indiana University, Bloomington, IN 47405, USA. Tel: +1-812-855-4922; fax: +1-812-855-4691.

E-mail: wellman@c@indiana.edu (C. L. Wellman).

Abbreviations: AchE, acetylcholinesterase; AMPA, α -amino-3-hydroxy-5-methylisoxazole-4-propionate; IPB, 0.1 M phosphate buffer, pH 7.4, plus 1% bovine serum albumin and 0.1% Triton X-100; NBM, nucleus basalis magnocellularis; NMDA, *N*-methyl-D-aspartate; PBS, phosphate-buffered saline.

(e.g. Nicoll and Malenka, 1999; Shi et al., 1999) and dendritic spines (e.g. Maletic-Savatic et al., 1999) associated with LTP depends on activation of NMDA receptors. Thus, the upregulation of dendritic spines and AMPA receptor protein in layer II–III neurons resulting from cholinergic deafferentation (Harmon and Wellman, 2003; Kim et al., 2005) may be mediated in part by NMDA receptors. To begin to test this hypothesis, we assessed the effect of NMDA receptor blockade on GluR1 expression and dendritic spine density on neurons in layer II–III of frontal cortex after lesion of the NBM.

EXPERIMENTAL PROCEDURES

Animals

The effect of NMDA receptor blockade on cholinergic lesion-induced increases in GluR1 subunit protein expression and dendritic spine density was assessed in young adult male Fischer 344 rats (3 months old; $N=47$). Throughout the experiment, rats were group-housed in cages equipped with filter tops. All experimental procedures were approved by the Bloomington Institutional Animal Care and Use Committee and carried out in accordance with NIH guidelines. Appropriate efforts were made to minimize the number and suffering of animals used.

Surgery

Rats were anesthetized with chloralpent (0.35 ml/100 g i.p.) and received either unilateral cholinergic lesions of the NBM using the immunotoxin 192 IgG-saporin (RBI; Natick, MA, USA) or unilateral sham lesions as described previously (Harmon and Wellman, 2003; Kim et al., 2005). Infusion of 192 IgG-saporin destroys cholinergic neurons of the NBM while leaving adjacent structures and noncholinergic neurons intact (Berger-Sweeney et al., 1994; Torres et al., 1994; Wenk et al., 1994). Each rat was placed in a stereotaxic instrument (Kopf; Tujunga, CA, USA) with the incisor bar set so that bregma and lambda were in the same horizontal plane. The scalp was incised and retracted, a hole was drilled, and the unilateral immunolesion was made at 0.8 mm posterior, 3.1 mm lateral, and 8.0 mm ventral to bregma (coordinates taken from the atlas of Paxinos and Watson, 1998). A cannula attached to a Hamilton microsyringe was lowered to the appropriate stereotaxic coordinates and left in place for 2 min prior to injection. 192 IgG-saporin (0.3 μ l, 0.5 μ g/ μ l) was pressure-injected in 0.1 μ l steps at 1 min intervals, and the cannula was slowly withdrawn 5 min after the final injection. To produce sham lesions, a cannula was lowered to the appropriate stereotaxic coordinates and withdrawn after 5 min. In addition, an osmotic minipump (Alzet, Model 2002; Roanoke, VA, USA) was implanted s.c. in the subscapular region of each rat. Half of the rats in each group received minipumps containing phosphate-buffered saline (PBS, pH 7.4); the other half received the noncompetitive NMDA antagonist MK-801 (6 mg/ml; Sigma; St. Louis, MO, USA). All pumps delivered solution at a rate of 0.5 μ l/h, yielding a dosage of approximately 0.1 mg/kg/h. Similar dosages of MK-801 have been demonstrated to have a variety of central effects, including influences on locomotor activity (Haggerty and Brown, 1996; Melani et al., 1999; Hutson et al., 2000) and striatal adenosine release (Melani et al., 1999).

Two weeks after surgery, rats were killed and their brains were processed for either immunohistochemical staining of the GluR1 subunit of the AMPA receptor (sham+PBS, $n=3$; sham+MK-801, $n=3$; lesion+PBS, $n=3$; lesion+MK-801, $n=4$) or Golgi histology (sham+PBS, $n=8$; sham+MK-801, $n=8$; lesion+PBS, $n=9$; lesion+MK-801, $n=9$).

Immunohistochemistry and GluR1-immunopositive neuron counts

Immunohistochemical labeling of the GluR1 subunit of the AMPA receptor was performed using a procedure similar to that of Kondo et al. (1997; see Fig. 1). Two weeks after surgery, each rat was deeply anesthetized with urethane and transcardially perfused with cold PBS (pH 7.4), followed by 4% paraformaldehyde in 0.1 M phosphate buffer (pH 7.4). The brain was removed, post-fixed for 2 h, and cryoprotected in 20% sucrose in 0.1 M phosphate buffer (pH 7.4). Frozen sections were cut coronally at 30 μ m on a sliding microtome. For each brain, three series of equally spaced sections (saving ratio 1:8) from the anterior portion of the claustrum through the dorsal hippocampus were saved. One series was then processed free-floating for immunohistochemistry, while the other two series were processed for lesion verification (see below). After rinsing in 0.1 M phosphate buffer (pH 7.4) containing 1% bovine serum albumin and 0.1% Triton X-100 (IPB), sections were incubated in IPB containing 4% normal goat serum to block nonspecific binding and 0.5% H_2O_2 to block endogenous peroxidase activity. Sections were then incubated overnight at 4 °C in IPB containing 1% normal goat serum plus a polyclonal antibody to the GluR1 subunit of the AMPA receptor (1:500; Chemicon International; Temecula, CA, USA). After rinsing in IPB, sections were incubated 1 h in IPB containing 4% normal goat serum and biotinylated goat anti-rabbit IgG (1:200; Vector; Burlingame, CA, USA). After rinsing in 0.1 M phosphate buffer (pH 7.4), sections were incubated in phosphate buffer with ABC Complex (Vector) 1 h. Staining was visualized using a nickel-intensified DAB reaction. After a final rinse, sections were mounted on chrome-alum subbed slides, dehydrated, cleared, and coverslipped. Control sections incubated without the primary antibody were generated and demonstrated virtually no staining.

Because we have previously shown effects of cholinergic deafferentation on AMPA receptor protein expression in layer II–III neurons in frontal cortex (Kim et al., 2005), GluR1 subunit protein expression was assessed in layer II–III neurons of frontal cortex. To quantify differences in GluR1 subunit protein expression, an unbiased stereological technique was used to estimate densities of labeled neurons. This technique has previously been demonstrated to be sensitive to changes in glutamatergic receptor protein expression as a result of either aging (Kim et al., 2005), cholinergic deafferentation (Kim et al., 2005), or differential environmental complexity (Wood et al., 2005). For each animal, one sample was taken in each of five sections per animal evenly spaced within the anterior–posterior axis. Within each section, the position of each sampling area within the Fr1–3 area of frontal cortex (nomenclature of Zilles and Wree, 1995) was randomly selected. For each section, the average optical density of the white matter in a 150 μ m \times 115 μ m area directly below the Fr1–3 area of frontal cortex (nomenclature of Zilles and Wree, 1995) was determined using a computerized image analysis system (Stereoinvestigator; MicroBrightField; Williston, VT, USA) interfaced with a microscope (Olympus BH-2; Mellville, NY, USA) at a final magnification of 1400 \times . Optical density of each areal sample was expressed as average luminosity per pixel within that sample, with luminosity ranging from 0 (black) to 256 (white). For each section, neurons with optical densities at least 1 standard deviation below this mean were then identified using the thresholding function of the image analysis system; these were considered intensely labeled and counted as described below, with the experimenter blind to condition.

The numerical densities of GluR1-immunopositive neurons were obtained using an optical disector procedure similar to that of Srivastava et al. (1993). Shrinkage of sections due to immunohistochemical processing was measured by focusing through each section with a 100 \times oil-immersion objective and measuring the distance traveled using a stage-mounted microcator calibrated to

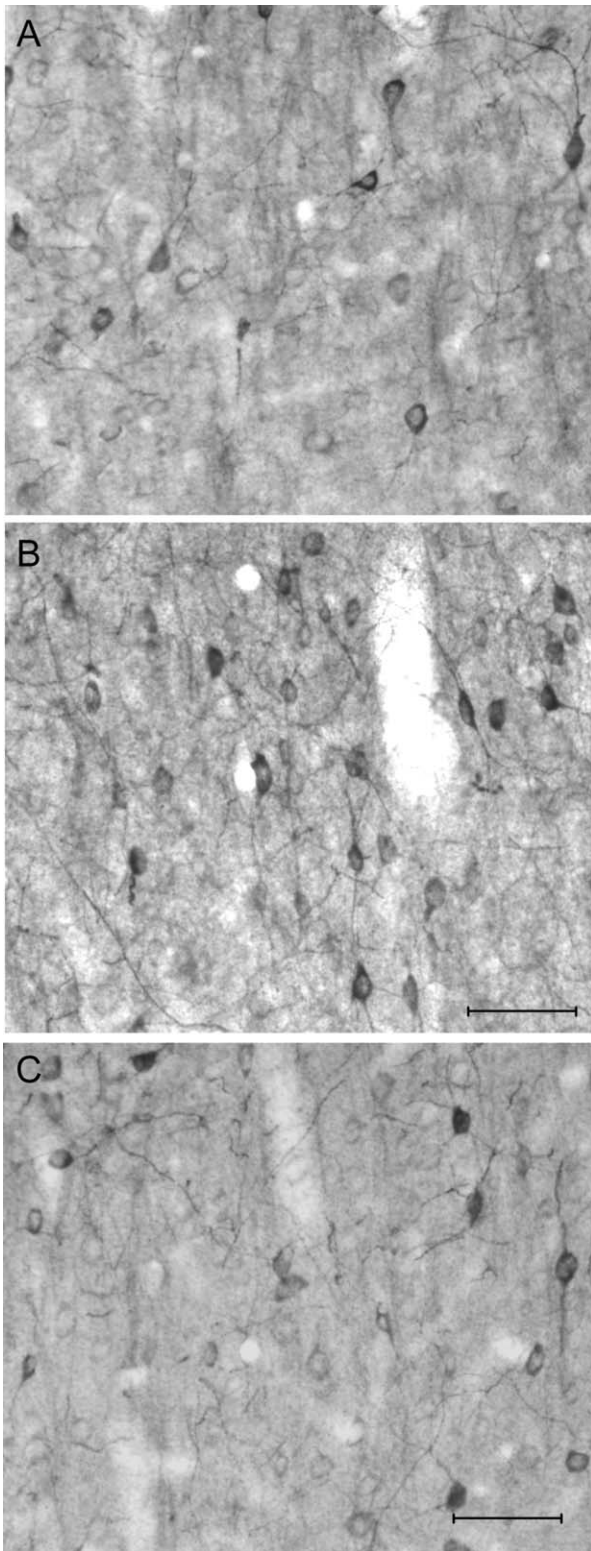


Fig. 1. Digital light micrographs of GluR1-immunopositive cells in frontal cortex in a sham-lesioned rat receiving PBS (A), a 192 IgG-saporin-lesioned rat receiving PBS (B), and a 192 IgG-saporin-lesioned rat receiving MK-801 (C). While all demonstrate robust cytoplasmic and dendritic staining of large numbers of neurons, an increase in intensely stained neurons is apparent in the lesion+PBS rat. Scale bar=50 μm .

a known standard. As in our previous study (Kim et al., 2005), shrinkage averaged $56.03 \pm 2.40\%$; thus, the length of the disector was 13 μm . This length was adequate for visualizing neurons in multiple focal planes (see Kim et al., 2005). For each section, counts were made at a final magnification of $1400\times$ in layer II–III of the Fr1–3 area within a $150 \mu\text{m} \times 115 \mu\text{m}$ grid and unbiased counting frame (i.e. neuronal somata touching the lower and left edge of the frame were not counted) whose medial–lateral position within the Fr1–3 area was randomly selected. Cells were identified as neurons based on standard morphological criteria (large, multipolar cell body; small, oval, homogeneously labeled cells were considered glia and therefore excluded). Neurons in the first focal plane (“tops”) were not counted (Coggeshall, 1992; West, 1993). Neuronal counts were divided by the volume of the counting frame ($150 \mu\text{m} \times 115 \mu\text{m} \times 13 \mu\text{m}$) and densities expressed as neurons per mm^3 . These estimates were averaged across the five samples within animals.

The volume of layer II–III was estimated using a computer-based image analysis system (MCID; Imaging Research, St. Catharines, Ontario, Canada). The area of layer II–III was measured in GluR1-labeled sections spaced evenly throughout the Fr1–3 area. Boundaries of the Fr1–3 area were determined based on its characteristic laminar structure and staining, which is apparent in GluR1-immunolabeled tissue (see Kim et al., 2005). Lamina boundaries are similarly readily identifiable. Volumes were then calculated using the Cavalieri estimator (Rosen and Harry, 1990). Estimates of total numbers of GluR1-immunolabeled neurons were obtained by multiplying average neuron densities by this volume.

Potential lesion and drug effects on estimated number of GluR1-immunopositive neurons were assessed using a two-way ANOVA (lesion \times drug), followed by appropriate planned comparisons. Planned comparisons consisted of *F* tests done within the context of the overall ANOVA (Hays, 1994).

Golgi histology and spine counts

To visualize whole neurons and their processes, the rostral portion of each brain (from the olfactory bulb to approximately the level of the medial septum) was dissected and processed using Glaser and Van der Loos’ modified Golgi stain (Glaser and Van der Loos, 1981). The remainder of the brain was immersed in 4% paraformaldehyde and processed for lesion verification (see below).

The rostral forebrain was immersed in Golgi–Cox solution (a 1:1 solution of 5% potassium dichromate and 5% mercuric chloride diluted 4:10 with 5% potassium chromate). When staining was complete [14 days, determined in pilot animals by developing test sections at regular intervals and assessing the presence of dendrites trailing off into a series of dots; see Coleman and Flood (1987)], brains were dehydrated in 1:1 absolute ethanol/acetone (3 h), followed by absolute ethanol and then 1:1 ethanol/ether (30 min each). Brains were then infiltrated with a graded series of celloidins before being embedded in 8% celloidin [8% (w/v) paraloid in 1:1 absolute ethanol/ether]. Coronal sections were cut at 150 μm on a sliding microtome (Leica SM2000R; Nussloch, Germany). Free-floating sections were then alkalized in 18.7% ammonia, developed in Kodak D19, fixed in Kodak Rapid Fix (prepared as per package instructions with Solution B omitted), dehydrated through a graded series of ethanols, cleared in xylene, mounted, and coverslipped (see Glaser and Van der Loos, 1981).

Layer II–III pyramidal neurons in the Fr1–3 area of frontal cortex ipsilateral to either 192 IgG-saporin or sham lesions were identified based on the presence of a basilar dendritic tree, a distinct, single apical dendrite, and dendritic spines (Fig. 2). Spine density was assessed on second- and third-order basilar branches, as previous work has localized effects of cholinergic deafferentation to this portion of the arbor (Harmon and Wellman, 2003; Works et al., 2004). For each animal, spines were counted on branches sampled from 10 neurons; this number yielded a within-animal error of 10.34%, and thus was considered to provide

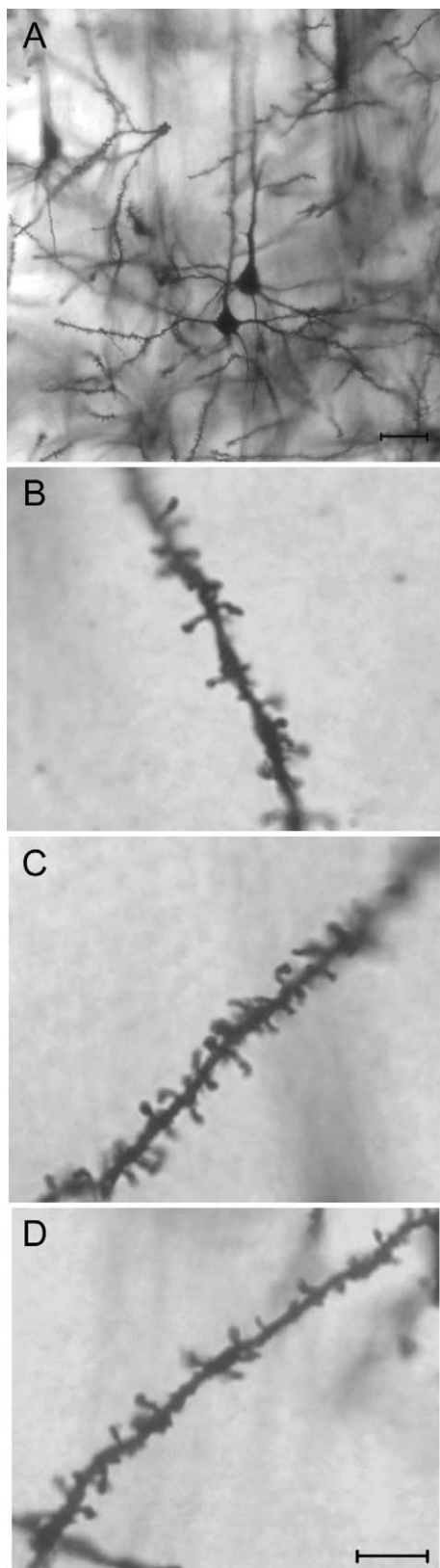


Fig. 2. (A) Digital light micrograph of Golgi-stained neurons in layer II–III of frontal cortex in a sham-lesioned rat receiving PBS. Scale bar=25 μm . (B–D) Photomicrographs showing spines on a second-

order basilar dendrite of a layer II–III pyramidal cell in frontal cortex. Neurons selected for analysis had somata in the upper half of the thickness of the section, and at least one basilar dendritic tree containing up to third-order dendrites that were not obscured by other branches or glial cells and extended relatively parallel to the plane of section. Within the population of neurons that met these criteria, neurons were selected from sections that were evenly distributed in the anterior–posterior axis between the forceps minor of the corpus callosum and the anterior commissure; the position of these neurons within the Fr1–3 area was randomly selected.

For each neuron, one basilar dendritic tree containing at least one second-order and one third-order dendrite was chosen. One to two branches at each order, averaging $32.09 \pm 2.00 \mu\text{m}$ in length, were drawn and spines counted at $1000\times$ using a computer-based morphometry system interfaced with a microscope (NeuroLucida, MicroBrightField), with the experimenter blind to condition. Spines were identified based on the morphological criteria for “mushroom” and “thin” spines described by Peters and Kaiserman-Abramof (1970): only protrusions perpendicular to the dendritic shaft and possessing a clear neck and bulbous head were counted (Fig. 2). These two spine types make up approximately 81% of the spine population in rat neocortex. Because spine density varies with thickness of the dendrite (and therefore branch order), the lengths of second- and third-order basilar dendrites were recorded, and spine densities (spines per $100 \mu\text{m}$) for each branch order were then calculated. Spine densities were compared across groups using three-way repeated-measures ANOVAs (lesion \times drug \times branch order), followed by appropriate planned comparisons. Planned comparisons consisted of *F* tests done within the context of the overall ANOVA (Hays, 1994).

Lesion verification

As in previous studies (Harmon and Wellman, 2003; Works et al., 2004; Kim et al., 2005), to verify extent and placement of lesions, two series of sections were mounted on gelatin-coated slides and either stained with Cresylecht Violet or processed for acetylcholinesterase (AChE) staining using a modification of the Karnovsky-Roots method (Hedreen et al., 1985).

To quantify the extent of the NBM lesions, AChE-positive fibers in frontal cortex were counted using a method similar to that of Stichel and Singer (1987) and a computer-based morphometry system interfaced with a microscope (NeuroLucida; MicroBrightField). A 5×5 counting grid consisting of $50 \mu\text{m}$ squares (for a total of $250 \times 250 \mu\text{m}$) was superimposed over the Fr1 area of frontal cortex ipsilateral to the lesion and perpendicular to the pial surface in the middle of layer II–III, in which we have previously documented age-dependent changes after NBM lesions (Wellman and Sengelau, 1995; Harmon and Wellman, 2003; Works et al., 2004; Kim et al., 2005). The number of crossings of fibers on the grid was then counted at $200\times$. For each rat, counts were made in each of three sections and averaged across samples. Density of AChE-positive fibers was expressed as number of fibers per counting grid, and compared across groups using a two-way ANOVA (lesion \times drug).

RESULTS

Lesion verification

Examination of Cresylecht Violet-stained sections revealed cannula tracts extending into the region of the

order basilar dendrite of a layer II–III pyramidal cell in frontal cortex of a sham-lesioned rat receiving PBS (B), a 192 IgG-saporin-lesioned rat receiving PBS (C), and a 192 IgG-saporin-lesioned rat receiving MK-801 (D). Scale bar=10 μm .

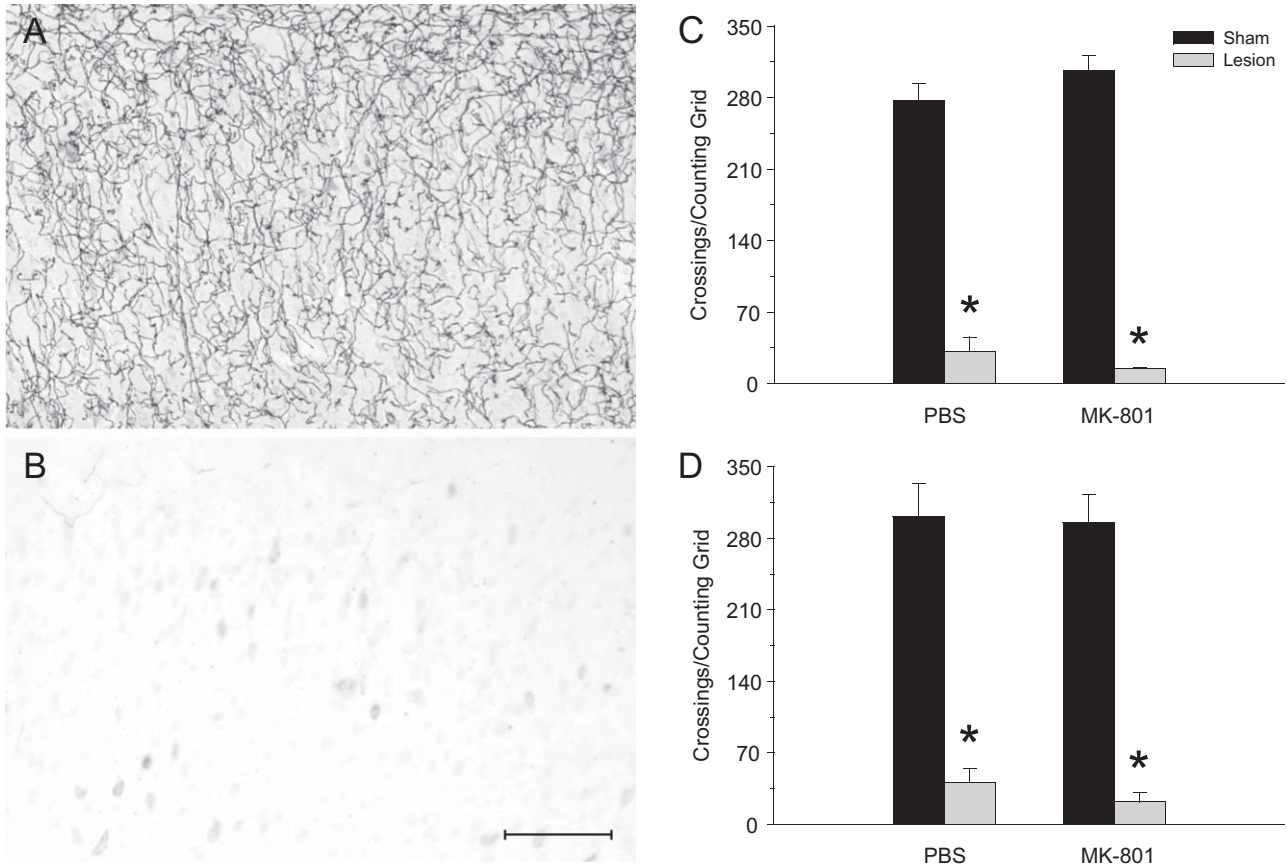


Fig. 3. (A, B) Digital light micrographs of AChE-stained fibers in frontal cortex of a sham- (A) and a 192 IgG-saporin-lesioned (B) rat. Reduction in staining is apparent. Scale bar=100 μ m. (C, D) Average density of AChE-positive fibers (expressed as average number of fiber crossings per counting grid) in layer II–III of frontal cortex ipsilateral to sham and 192 IgG-saporin lesions of the NBM in rats receiving PBS or MK-801. Lesions produced a profound reduction in AChE staining in both PBS- and MK-801-treated rats. Vertical bars represent S.E.M. values; asterisks (*) indicate significant difference relative to sham+PBS rats.

NBM, and visual inspection revealed an absence of magnocellular neurons in the basal forebrain in all of the 192 IgG-saporin-lesioned rats. In addition, for animals used for immunohistochemistry, lesions significantly reduced AChE-stained fibers in frontal cortex by approximately 92% [$F(1,9)=516.16$, $P<0.01$], and this effect was uniform across the drug treatment conditions [lesion \times drug interaction, $F(1,9)=3.81$, ns]. MK-801 administration had no effect on AChE-stained fibers [$F(1,9)=0.27$, ns]. The average number of AChE-positive fibers per counting grid was 277.39 ± 16.70 S.E.M. for sham+PBS rats, 31.61 ± 13.79 S.E.M. for lesion+PBS rats, 306.67 ± 14.19 S.E.M. for sham+MK-801 rats, and 14.67 ± 1.01 S.E.M. for lesion+MK-801 rats. Similarly, for animals used for Golgi histology, lesions significantly reduced AChE-stained fibers in frontal cortex by approximately 89% [$F(1,30)=152.64$, $P<0.01$], and this effect was uniform across treatment conditions [lesion \times drug interaction, $F(1,30)=0.11$, ns]. MK-801 administration had no effect on AChE-stained fibers [$F(1,30)=0.32$, ns]. The average number of AChE-positive fibers per counting grid was 300.91 ± 32.54 S.E.M. for sham+PBS rats, 41.33 ± 13.34 S.E.M. for lesion+PBS rats, 295.79 ± 26.93 S.E.M. for sham+MK-801 rats, and 22.06 ± 8.87

S.E.M. for lesion+MK-801 rats. Thus, lesions produced a profound reduction in cholinergic innervation across all groups (Fig. 3).

Immunohistochemical analysis

Stereological information. Average optical density of the white matter samples was 251.28 ± 4.43 S.E.M. The average number of objects counted per frame was 26.25 ± 0.96 S.E.M., and the total number of objects counted across the five frames averaged 131.25 ± 4.80 . Within-subjects error for neuronal densities averaged $3.57\%\pm 0.51\%$. Overall, the average volume of frontal cortex was unaffected by lesion [$F(1,9)=2.96$, ns] or by drug [$F(1,9)=1.43$, ns]; there was also no interaction of lesion and drug [$F(1,9)=0.84$, ns].

GluR1-immunopositive neuron counts. To assess the ability of MK-801 to block the lesion-induced increase in expression of the GluR1 subunit protein, the average number of intensely stained immunopositive neurons was compared across groups (see Figs. 1 and 4). Two-way ANOVA indicated significant effects of both lesion [$F(1,9)=9.52$, $P<0.05$] and drug [$F(1,9)=7.98$, $P<0.05$] on the number of intensely stained neurons. In addition, there

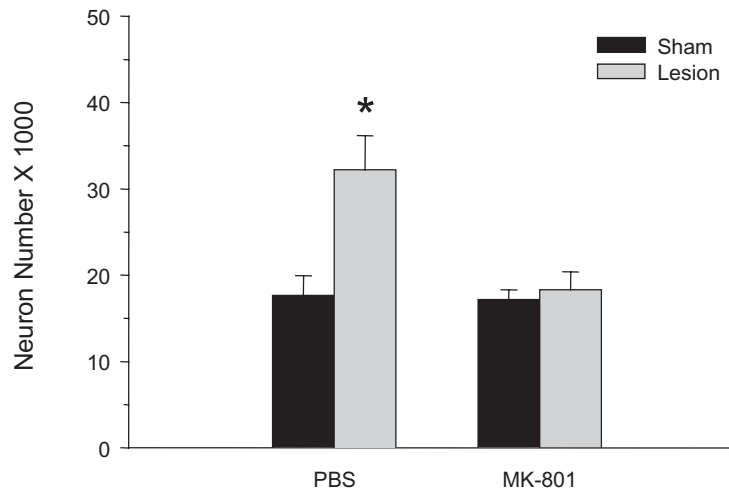


Fig. 4. Average number of intensely stained GluR1-positive neurons in layer II–III of frontal cortex ipsilateral to sham and 192 IgG-saporin lesions of the NBM in rats receiving PBS or MK-801. MK-801 blocked the lesion-induced increase in GluR1 expression. Vertical bars represent S.E.M. values; asterisk (*) indicates significant difference relative to sham+PBS rats.

was a significant interactive effect of lesion and drug [$F(1,9)=6.98$, $P<0.05$].

Planned comparisons indicated that the number of intensely stained neurons was increased approximately 83% in lesion+PBS rats compared with sham+PBS rats [$F(1,4)=10.11$, $P<0.05$]. Furthermore, the number of intensely stained GluR1-immunopositive neurons did not differ significantly in sham+MK-801 rats relative to sham+PBS rats [$F(1,4)=0.03$, ns]. In addition, the number of intensely stained neurons in lesion+PBS rats was significantly higher than in lesion+MK-801 rats [$F(1,5)=11.24$, $P<0.05$]. On the other hand, there was no significant difference in number of intensely stained GluR1-immunopositive neurons between lesion+MK-801 rats and sham+PBS rats [$F(1,5)=0.05$, ns].

Dendritic spine density analysis

In all treatment groups, complete impregnation of numerous cortical pyramidal neurons was apparent (Fig. 2), and layer II–III was readily identifiable. Spine density varied significantly with lesion [main effect of lesion, $F(1,30)=5.25$, $P<0.03$; see Figs. 2 and 5], and this effect was consistent across branch orders [for lesion \times branch order interaction, $F(1,30)=1.75$, ns]. Furthermore, there was no effect of MK-801 treatment alone [$F(1,30)=0.17$, ns] at either branch order [for drug \times branch order interaction, $F(1,30)=0.70$, ns]. However, there was an interactive effect of lesion and drug on spine density [$F(1,30)=4.35$, $P<0.05$], which was consistent across branch orders [for lesion \times drug \times branch order interaction, $F(1,30)=0.12$, ns].

Planned comparisons demonstrated that NBM lesions increased spine density on both second- and third-order branches by 30% and 25%, respectively [for second-order branches, $F(1,15)=8.36$, $P<0.01$; for third-order branches, $F(1,15)=7.90$, $P<0.01$]. MK-801 administration prevented this lesion-induced increase: for second-order branches, the difference in spine density between the lesion+PBS and lesion+MK-801 rats approached significance [$F(1,16)=3.83$,

$P<0.07$], while for third-order branches this difference was significant [$F(1,16)=4.47$, $P<0.05$]. Additionally, comparison of the sham+PBS and lesion+MK-801 rats showed no significant difference at either branch order [second-order branches, $F(1,15)=1.52$, ns; third-order branches, $F(1,15)=1.22$, ns].

DISCUSSION

The present study demonstrated parallel effects of cholinergic deafferentation on expression of the GluR-1 subunit of the AMPA receptor and dendritic spines in frontal cortex. As previously demonstrated (Kim et al., 2005), lesions of the NBM increased GluR1 expression in neurons in layer II–III of frontal cortex. This effect was quite robust, with a near-doubling of intensely labeled neurons in the lesion+PBS group that was statistically significant despite small group n 's. Similarly, NBM lesions increased spine density on layer II–III pyramidal neurons in frontal cortex, replicating a previous finding (Harmon and Wellman, 2003). Furthermore, the present results indicate that these effects are NMDA receptor-mediated: while administration of the noncompetitive NMDA channel blocker MK-801 alone had no effect on either GluR1 expression or spine density, it prevented the lesion-induced increases in GluR1 expression and spine density. This effect was not due to either sparing or sprouting of cholinergic afferents from the NBM, as MK-801 administration did not significantly alter AChE staining in frontal cortex in saporin-lesioned animals.

The present finding is consistent with previous studies demonstrating a critical role for NMDA receptors in synaptic plasticity (e.g. Artola and Singer, 1987; Garraghty and Muja, 1996; Maletic-Savatic et al., 1999; Shi et al., 1999). Furthermore, the present finding supports previous data suggesting a role for cholinergic-glutamatergic interactions in synaptic plasticity. For instance, previous studies have demonstrated that repeated combined iontophoretic applica-

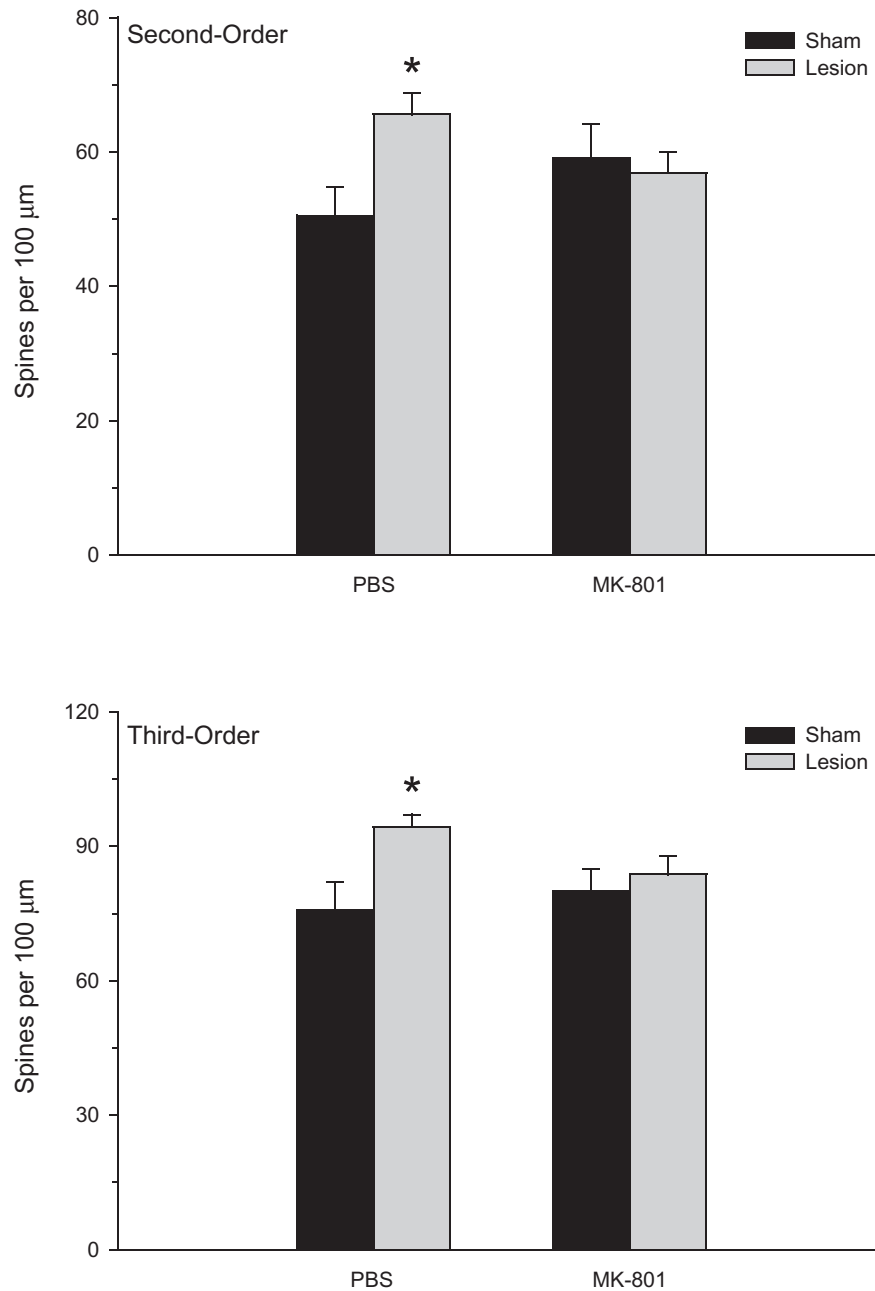


Fig. 5. Mean spine density on second- (top) and third-order (bottom) basilar branches on pyramidal neurons in layer II–III of frontal cortex ipsilateral to sham and 192 IgG-saporin lesions of the NBM in rats receiving PBS or MK-801. MK-801 blocked the lesion-induced increase in spine density. Vertical bars represent S.E.M. values; asterisks (*) indicate significant difference relative to sham+PBS rats.

tion of glutamate and acetylcholine increases the thickness of postsynaptic densities in axodendritic synapses in rat sensorimotor cortex, while muscarinic receptor blockade prevents this effect (Khludova and Gusev, 1999). In addition, activation of nicotinic receptors facilitates NMDA-dependent LTP in hippocampal area CA1 (Ji et al., 2001; Ge and Dani, 2005). Finally, previous data from our laboratory demonstrate cholinergic influences on AMPA receptor protein expression (Kim et al., 2005), and the present results implicate NMDA receptors in this effect.

Because MK-801 was administered systemically in the present study, the site of action of this effect cannot be determined. Thus, MK-801 may be preventing the lesion-induced increase in GluR1 expression and spine density in layer II–III of frontal cortex either directly, by decreasing efficacy of transmission at NMDA receptors on neurons with AMPA receptors containing GluR1 subunits, or indirectly, by decreasing efficacy of transmission at NMDA receptors on an alternate population of cells. For instance, while iontophoretic application of acetylcholine directly onto cortical pyramidal neurons alters their response to

glutamate (e.g. Metherate et al., 1987; Tremblay et al., 1990a), cholinergic fibers also synapse on glutamatergic axons in cortex (e.g. Marchi et al., 2002) and stimulate release of glutamate. In addition, application of cholinergic agonists in a cortical slice preparation activates inhibitory interneurons (Kondo and Kawaguchi, 2001). Thus, the critical site of the cholinergic-NMDA interaction could be either presynaptic, on inhibitory interneurons, or on pyramidal neurons.

Furthermore, in the present study, we have quantified changes in expression of GluR1 localized in neuronal somata. While the distribution of intracellular pools of AMPA receptor subunits in dendrites has been shown to be correlated with the distribution of AMPAergic synapses (Rubio and Wenthold, 1999), changes in somal expression could reflect changes in some aspect of synthesis or storage that is unrelated to the number of functional synapses. Future studies examining cholinergic-NMDA interactions in GluR1 surface expression would further clarify this issue.

Another consideration is that the design of this study, in which changes in GluR1 immunolabeling and spine density were assessed at only one time point post-lesion, prevents an assessment of the exact role of NMDA receptors in this plasticity. The data are consistent with the hypothesis that MK-801 prevents the upregulation of GluR1 expression in layer II–III of frontal cortex in young adult rats after NBM lesion. Alternatively, the time course of cortical neurons' response to cholinergic deafferentation may simply be slowed by NMDA receptor blockade. It is possible that at a later time point, GluR1 expression and spine density in lesioned rats who received MK-801 may reach the magnitude seen in lesioned rats who received PBS. Examination of the time course of the interactive effects of MK-801 administration and NBM lesion on GluR1 expression and spine density in frontal cortex would determine whether NMDA receptor blockade attenuates or simply slows GluR1 and spine upregulation.

The NMDA receptor-blockade alterations in GluR1 expression and spine density documented here have implications for both basic mechanisms of synaptic plasticity and alterations in plasticity that may occur with either aging or pathology. Dendritic spines are the principal site of excitatory input in the neocortex (Gray, 1959), and are thought to play an important role in neuronal information processing (Hering and Sheng, 2001). In addition, spine structure and number are modified by activity (e.g. Chang and Greenough, 1984; Andersen et al., 1987a,b; Trommald et al., 1990, 1996; Moser et al., 1997), and may therefore provide a morphological substrate for synaptic plasticity induced by experience, alterations in activity, or afferent innervation (Hering and Sheng, 2001). We have previously demonstrated that plasticity of frontal cortex is altered in aging rats: lesions of the NBM fail to significantly increase either GluR1 expression or dendritic spine density in frontal cortex of middle-aged and aged rats (Kim et al., 2005). Others have shown that NMDA receptors are reduced in aged cortex. Interestingly, numerous studies have demonstrated decreased NMDA receptor binding in frontal cortex of aged rats (Tamaru et al., 1991; Wenk et

al., 1991; Castorina et al., 1994; Mitchell and Anderson, 1998), mice (Magnusson, 2000), and monkeys (Wenk et al., 1991). The present data are consistent with the hypothesis that decreased efficacy of transmission at NMDA receptors in frontal cortex is responsible for the attenuated increase in GluR1 expression and spine density in layer II–III of frontal cortex following cholinergic deafferentation in middle-aged and aged rats. If this is the case, then administration of an NMDA facilitator, such as the partial agonist D-cycloserine, should restore the lesion-induced increase in GluR1 expression and spine density in layer II–III of frontal cortex following cholinergic deafferentation in middle-aged and aged rats.

Finally, NBM lesions produce differential cognitive effects in young versus aged rats. For instance, cholinergic deafferentation of prefrontal cortex in young adult rats produces relatively minimal attentional deficits immediately following the lesions; however, attentional deficits become apparent as the animals age (Burk et al., 2002). Similarly, NBM lesions produce more pronounced deficits in radial arm maze performance in aged rats compared with young adults (Wellman and Pellemounter, 1999). Thus, NMDA-receptor-mediated up-regulation of GluR1 expression and dendritic spines in young adult rats may be a compensatory response that minimizes the functional impact of cholinergic deafferentation; attenuation of this compensatory response may be responsible for the cognitive deficits induced by cholinergic lesions in aged rats. If this is the case, then MK-801 blockade in young adult rats should amplify the cognitive deficits produced by cholinergic deafferentation, whereas administration of an NMDA facilitator in aging lesioned rats should attenuate lesion-induced cognitive deficits.

Acknowledgments—We thank Michael F. Brace, Sarah M. Brown, and Kellie D. Huyck for their excellent technical assistance and Dr. Dale R. Sengelaub for his helpful comments on the manuscript. This research was supported by NIH-NIA P30AG10133 to C.L.W.

REFERENCES

- Andersen P, Blackstad T, Hulleberg G, Trommald M, Vaaland JL (1987a) Changes in spine morphology associated with LTP in rat dentate granule cells. *Proc Physiol Soc PC50*:P288.
- Andersen P, Blackstad T, Hulleberg G, Trommald M, Vaaland JL (1987b) Dimensions of dendritic spines of rat dentate granule cells during long-term potentiation. *J Physiol* 390:P264.
- Artola A, Singer W (1987) Long-term potentiation and NMDA receptors in rat visual cortex. *Nature* 330:649–652.
- Berger-Sweeney J, Heckers S, Mesulam M-M, Wiley RG, Lappi DA, Sharma M (1994) Differential effects on spatial navigation of immunotoxin-induced cholinergic lesions of the medial septal area and nucleus basalis magnocellularis. *J Neurosci* 14:4507–4519.
- Bigl V, Woolf NJ, Butcher LL (1982) Cholinergic projections from the basal forebrain to frontal, parietal, temporal, occipital, and cingulate cortices: a combined fluorescent tracer and acetylcholinesterase analysis. *Brain Res Bull* 8:727–749.
- Burk JA, Herzog CD, Porter MC, Sarter M (2002) Interactions between aging and cortical cholinergic deafferentation on attention. *Neurobiol Aging* 23:467–477.
- Castorina M, Ambrosini AM, Pacifici L, Ramacci MT, Angelucci L (1994) Age-dependent loss of NMDA receptors in hippocampus, striatum,

- and frontal cortex of the rat: prevention by acetyl-L-carnitine. *Neurochem Res* 19:795–798.
- Chang FLF, Greenough WT (1984) Transient and enduring morphological correlates of synaptic activity and efficacy change in the rat hippocampal slice. *Brain Res* 309:35–46.
- Coggeshall RE (1992) A consideration of neural counting methods. *Trends Neurosci* 15:9–13.
- Coleman PD, Flood DG (1987) Neuron numbers and dendritic extent in normal aging and Alzheimer's disease. *Neurobiol Aging* 8: 521–545.
- Garraghty PE, Muja N (1996) NMDA receptors and plasticity in adult primate somatosensory cortex. *J Comp Neurol* 367:319–326.
- Ge S, Dani JA (2005) Nicotinic acetylcholine receptors at glutamate synapses facilitate long-term depression or potentiation. *J Neurosci* 25:6084–6091.
- Glaser EM, Van der Loos H (1981) Analysis of thick brain sections by obverse-reverse computer microscopy: application of a new, high-quality Golgi-Nissl stain. *J Neurosci Methods* 4:117–125.
- Gray EG (1959) Axosomatic and axodendritic synapses of the cerebral cortex: an electron microscopic study. *J Anat* 83:420–433.
- Haggerty GC, Brown G (1996) Neurobehavioral profile of subcutaneously administered MK-801 in the rat. *Neurotoxicology* 17:913–921.
- Harmon KM, Wellman CL (2003) Differential effects of cholinergic lesions on dendritic spines in frontal cortex of young adult and aging rats. *Brain Res* 992:60–68.
- Hays WL (1994) *Statistics*. Fort Worth, TX: Harcourt Brace.
- Hedreen JC, Bacon SJ, Price DL (1985) A modified histochemical technique to visualize acetylcholinesterase-containing axons. *J Histochem Cytochem* 33:134–140.
- Hering H, Sheng M (2001) Dendritic spines: structure, dynamics, and regulation. *Nat Rev Neurosci* 2:880–888.
- Hess G, Donoghue JP (1999) Facilitation of long-term potentiation in layer II/III horizontal connections of rat motor cortex following layer I stimulation: route of effect and cholinergic contributions. *Exp Brain Res* 127:279–290.
- Hohmann CF, Brooks AR, Coyle JT (1988) Neonatal lesions of the basal forebrain cholinergic neurons result in abnormal cortical development. *Dev Brain Res* 42:253–264.
- Hutson PH, Barton CL, Jay M, Blurton P, Burkamp F, Clarkson R, Bristow LJ (2000) Activation of mesolimbic dopamine function by phencyclidine is enhanced by 5-HT_{2C/2B} receptor antagonists: neurochemical and behavioural studies. *Neuropharmacology* 39:2318–2328.
- Inglis FM, Crockett R, Korada S, Abraham WC, Hollmann M, Kalb RG (2002) The AMPA receptor subunit GluR1 regulates dendritic architecture of motor neurons. *J Neurosci* 22:8042–8051.
- Ji D, Lape R, Dani JA (2001) Timing and location of nicotinic activity enhances or depresses hippocampal synaptic plasticity. *Neuron* 31:131–141.
- Johnston MV, McKinney M, Coyle JT (1981) Neocortical cholinergic innervation: a description of extrinsic and intrinsic components in the rat. *Exp Brain Res* 43:159–172.
- Juliano SL, Ma W, Eslin D (1991) Cholinergic depletion prevents expansion of topographic maps in somatosensory cortex. *Proc Natl Acad Sci U S A* 88:780–784.
- Kennedy MB (2000) Signal-processing machines at the postsynaptic density. *Science* 290:750–754.
- Khludova GG, Gusev PA (1999) The effects of atropine on associative-type ultrastructural postsynaptic plasticity in the rat neocortex. *Neurosci Behav Physiol* 29:727–729.
- Kim I, Wilson RE, Wellman CL (2005) Aging and cholinergic deafferentation alter GluR1 expression in rat frontal cortex. *Neurobiol Aging* 26:1073–1081.
- Kondo M, Sumino R, Okado H (1997) Combinations of AMPA receptor subunit expression in individual cortical neurons correlate with expression of specific calcium-binding proteins. *J Neurosci* 17:1570–1581.
- Kondo S, Kawaguchi Y (2001) Slow synchronized bursts of inhibitory postsynaptic currents (0.1–0.3 Hz) by cholinergic stimulation in the rat frontal cortex in vitro. *Neuroscience* 107:551–560.
- Kurosawa M, Sato A, Sato Y (1989) Stimulation of the nucleus basalis of Meynert increases acetylcholine release on the cerebral cortex in rats. *Neurosci Lett* 98:45–50.
- Magnusson KR (2000) Declines in mRNA expression of different subunits may account for differential effects of aging on agonist and antagonist binding to the NMDA receptor. *J Neurosci* 20: 1666–1674.
- Maletic-Savatic M, Malinow R, Svoboda K (1999) Rapid dendritic morphogenesis in CA1 hippocampal dendrites induced by synaptic activity. *Science* 283:1923–1926.
- Marchi M, Risso F, Viola C, Cavazzani P, Raiteri M (2002) Direct evidence that release-stimulating $\alpha 7^*$ nicotinic cholinergic receptors are localized on human and rat brain glutamatergic axon terminals. *J Neurochem* 80:1071–1078.
- Mattson MP, Dou P, Kater SB (1988) Outgrowth-regulating actions of glutamate in isolated hippocampal pyramidal neurons. *J Neurosci* 8:2087–2100.
- Melani A, Corsi C, Giménez-Llort L, Martínez E, Ove Ögren S, Pedata F, Ferré S (1999) Effect of *N*-methyl-D-aspartate on motor activity and in vivo adenosine striatal outflow in the rat. *Eur J Pharmacol* 385:15–19.
- Metherate R, Tremblay N, Dykes RW (1987) Acetylcholine permits long-term enhancement of neuronal responsiveness in cat primary somatosensory cortex. *Neuroscience* 22:75–81.
- Metzger F, Wiese S, Sendtner M (1998) Effect of glutamate on dendritic growth in embryonic rat motoneurons. *J Neurosci* 18:1735–1742.
- Mitchell JJ, Anderson KJ (1998) Age-related changes in [³H]MK-801 binding in the Fischer 344 rat brain. *Neurobiol Aging* 19:259–265.
- Moser MB, Trommald M, Egeland T, Andersen P (1997) Spatial training in a complex environment and isolation alter the spine distribution differently in rat CA1 pyramidal cells. *J Comp Neurol* 380:373–381.
- Nicoll RA, Malenka RC (1999) Expression mechanisms underlying NMDA receptor-dependent long-term potentiation. *Ann N Y Acad Sci* 868:515–525.
- Paxinos G, Watson C (1998) *The rat brain in stereotaxic coordinates*. New York: Academic Press.
- Peters A, Kaiserman-Abramof IR (1970) The small pyramidal neuron of the rat cerebral cortex. The perikaryon, dendrites and spines. *Am J Anat* 127:321–355.
- Puil E, Benjamin AM (1988) Functional organization of glutamatergic synapses. In: *Neurotransmitters and cortical function* (Avoli M et al., eds), pp 25–37. New York: Plenum.
- Rasmusson DD, Dykes RW (1988) Long-term enhancement of evoked potentials in cat somatosensory cortex produced by co-activation of the basal forebrain and cutaneous receptors. *Exp Brain Res* 70:276–286.
- Ricceri L, Hohmann C, Berger-Sweeney J (2002) Early neonatal 192 IgG saporin induces learning impairments and disrupts cortical morphogenesis in rats. *Brain Res* 954:160–172.
- Rosen GD, Harry JD (1990) Brain volume estimation from serial section measurements: A comparison of methodologies. *J Neurosci Methods* 35:115–125.
- Roßner S, Schleibs R, Bigl V (1995) 192IgG-saporin-induced immunotoxic lesions of cholinergic basal forebrain system differentially affect glutamatergic and GABAergic markers in cortical rat brain regions. *Brain Res* 696:165–176.
- Rubio ME, Wenthold RJ (1999) Differential distribution of intracellular glutamate receptors in dendrites. *J Neurosci* 19:5549–5562.
- Shi SH, Hayashi Y, Petralia RS, Zaman SH, Wenthold RJ, Svoboda K, Malinow R (1999) Rapid spine delivery and redistribution of AMPA receptors after synaptic NMDA receptor activation. *Science* 284: 1811–1816.
- Srivastava R, Brouillet E, Beal MF, Storey E, Hyman BT (1993) Blockade of 1-methyl-4-phenylpyridinium ion (MPP⁺) nigral toxicity in

- the rat by prior decortication or MK-801 treatment: a stereological estimate of neuronal loss. *Neurobiol Aging* 14:295–301.
- Stichel CC, Singer W (1987) Quantitative analysis of the choline acetyltransferase-immunoreactive axonal network in the cat primary visual cortex: I. Adult cats. *J Comp Neurol* 258:91–98.
- Tamaru M, Yoneda Y, Ogita K, Shimizu J, Nagata Y (1991) Age-related decreases of the *N*-methyl-D-aspartate receptor complex in the rat cerebral cortex and hippocampus. *Brain Res* 542:83–90.
- Torres EM, Perry TA, Blokland A, Wilkinson LS, Wiley RG, Lappi DA, Dunnett SB (1994) Behavioural, histochemical and biochemical consequences of selective immunolesions in discrete regions of the basal forebrain cholinergic system. *Neuroscience* 63:95–122.
- Tremblay N, Warren RA, Dykes RW (1990a) Electrophysiological studies of acetylcholine and the role of the basal forebrain in the somatosensory cortex of the cat. I. Cortical neurons excited by glutamate. *J Neurophysiol* 64:1199–1211.
- Tremblay N, Warren RA, Dykes RW (1990b) Electrophysiological studies of acetylcholine and the role of the basal forebrain in the somatosensory cortex of the cat. II. Cortical neurons excited by somatic stimuli. *J Neurophysiol* 64:1212–1222.
- Trommald M, Hulleberg G, Andersen P (1996) Long-term potentiation is associated with new excitatory spine synapses on rat dentate granule cells. *Learn Mem* 3:218–228.
- Trommald M, Vaaland JL, Blackstad T, Andersen P (1990) Dendritic spine changes in rat dentate granule cells associated with long-term potentiation. In: *Neurotoxicity of excitatory amino acids* (Guidotti A, ed), pp 163–174. New York: Raven.
- Webster HH, Hanisch UK, Dykes RW, Biesold D (1991) Basal forebrain lesions with or without reserpine injection inhibit cortical reorganization in rat hindpaw primary somatosensory cortex following sciatic nerve transection. *Somatosens Mot Res* 8:327–346.
- Wellman CL, Pelleymounter MA (1999) Differential effects of nucleus basalis lesions in young adult and aging rats. *Neurobiol Aging* 20:381–393.
- Wellman CL, Sengelaub DR (1995) Alterations in dendritic morphology of frontal cortical neurons after basal forebrain lesions in adult and aged rats. *Brain Res* 669:48–58.
- Wenk GL, Stoehr JD, Quintana G, Mobley S, Wiley RG (1994) Behavioral, biochemical, histological, and electrophysiological effects of 192 IgG-saporin injections into the basal forebrain of rats. *J Neurosci* 14:5986–5995.
- Wenk GL, Walker LC, Price DL, Cork LC (1991) Loss of NMDA, but not GABA-A, binding in the brains of aged rats and monkeys. *Neurobiol Aging* 12:93–98.
- West MJ (1993) New stereological methods for counting neurons. *Neurobiol Aging* 14:275–285.
- Wilson MT, Keith CH (1998) Glutamate modulation of dendrite outgrowth: alterations in the distribution of dendritic microtubules. *J Neurosci Res* 52:599–611.
- Wong WT, Faulkner-Jones BE, Sanes JR, Wong ROL (2000) Rapid dendritic remodeling in the developing retina: dependence on neurotransmission and reciprocal regulation by Rac and Rho. *J Neurosci* 20:5024–5036.
- Wood DA, Buse JE, Wellman CL, Rebec GV (2005) Differential environmental exposure alters NMDA but not AMPA receptor subunit expression in nucleus accumbens core and shell. *Brain Res* 1042:176–183.
- Works SJ, Wilson RE, Wellman CL (2004) Age-dependent effect of cholinergic lesion on dendritic morphology in rat frontal cortex. *Neurobiol Aging* 25:963–974.
- Zilles K, Wree A (1995) Cortex: areal and laminar structure. In: *The rat nervous system* (Paxinos G, ed), pp 649–685. San Diego: Academic Press.

(Accepted 26 January 2006)
(Available online 9 March 2006)